Mice deficient for the epidermal dermokine and isoforms display transient cornification defects

Emilie A. Leclerc, Anne Huchenq, S. Kezic, Guy Serre, Nathalie Jonca

© 2014. Published by The Company of Biologists Ltd | Journal of Cell Science (2014) 127, 2862–2872 doi:10.1242/jcs.144808

RESEARCH ARTICLE

Mice deficient for the epidermal dermokine β and γ isoforms display transient cornification defects

Emilie A. Leclerc[1], Anne Huchenq[1], Sanja Kezic[2], Guy Serre[1] and Nathalie Jonca[1,*]

ABSTRACT

Expression of the human dermokine gene (*DMKN*) leads to the production of four dermokine isoform families. The secreted α, β and γ isoforms have an epidermis-restricted expression pattern, with Dmkn β and γ being specifically expressed by the granular keratinocytes. The δ isoforms are intracellular and ubiquitous. Here, we performed an in-depth characterization of *Dmkn* expression in mouse skin and found an expression pattern that was less complex than in humans. In particular, mRNA coding for the δ family were absent. Homozygous mice null for the Dmkn β and γ isoforms had no obvious phenotype but only a temporary scaly skin during the first week of life. The pups null for the Dmkn β and γ isoforms had smaller keratohyalin granules and their cornified envelopes were more sensitive to mechanical stress. At the molecular level, amounts of profilaggrin and filaggrin monomers were reduced whereas amino acid components of the natural moisturizing factor were increased. In addition, the electrophoretic mobility of involucrin was modified, suggesting post-translational modifications. Finally, the mice null for the Dmkn β and γ isoforms strongly overexpressed Dmkn α. These data are evocative of compensatory mechanisms relevant to the temporary phenotype. Overall, we improved the knowledge of *Dmkn* expression in mouse and highlighted a role for Dmkn β and γ in cornification.

KEY WORDS: Cornified cell envelope, Dermokine, Dmkn, Keratinocyte differentiation, Stratum corneum

INTRODUCTION

Terminal differentiation of the epidermal keratinocytes corresponds to the expression of numerous genes orchestrating proliferation arrest and complex biochemical events associated with major morphological modifications. It takes place as keratinocytes migrate upwards through the spinous, granular and cornified layers of the epidermis, and culminates with cornification, a peculiar cell death program. A tightly regulated balance between proliferation in the basal compartment and desquamation at the external surface of the epidermis is essential for the tissue homeostasis and its protective barrier functions, mainly achieved by the *stratum corneum*.

[1]UMR 5165 / U1056 'Différenciation Epidermique et Autoimmunité Rhumatoïde' (CNRS – INSERM – Université Toulouse III – CHU de Toulouse), Hôpital Purpan, Place du Dr Baylac, TSA 40031, 31059 Toulouse Cedex 9, France. [2]Coronel Institute of Occupational Health, Academic Medical Center, 1105 Amsterdam, The Netherlands.

*Author for correspondence (nathalie.jonca@udear.cnrs.fr)

Received 18 October 2013; Accepted 8 April 2014

DMKN, encoding dermokine, was identified as one of the most highly expressed genes by the granular keratinocytes besides known late differentiation genes like *KRT1* and *FLG* (Matsui et al., 2004; Moffatt et al., 2004; Toulza et al., 2006). In humans, it is located at 19q13.1 within the 'stratified epithelium secreted peptides complex' (SSC) locus, and is surrounded by two other genes encoding proteins secreted in stratified epithelia, namely suprabasin (*SBSN*) (Park et al., 2002) and keratinocyte-differentiation associated protein (*KRTDAP*) (Tsuchida et al., 2004). *DMKN* is composed of 25 exons spanning 17 kb of genomic DNA. Two families of mRNAs produced by alternative splicing and encoding isoforms α and β were first described (Matsui et al., 2004). Identification of two additional families of splicing variants encoding DMKN γ and δ revealed a more complex pattern of expression, with the gene having three transcriptional start sites, two transcriptional termination sites and eight alternative coding exons (Toulza et al., 2006). The expression of the four isoform families is tissue-specific. The β and γ transcripts are specific to the epidermis, whereas mRNAs encoding DMKN α are detected in the placenta and the epidermis, and those encoding DMKN δ in most organs. Moreover, quantitative RT-PCR experiments revealed that the β and γ isoforms were highly and specifically expressed by the granular keratinocytes, whereas the α and δ isoforms were equally expressed in all epidermis layers (Toulza et al., 2004). Finally, the different DMKN isoforms differ in their subcellular location: α, β and γ are secreted, whereas δ is cytosolic. In the epidermis, DMKN β and γ are secreted by the lamellar bodies and detected in the intercellular space between the granular and the cornified layers of normal human epidermis (Toulza et al., 2006). There is little data about *DMKN* expression in human diseases; DMKN β and γ are overexpressed in inflammatory skin diseases, downregulated in skin cancers and, although hardly detected in normal colon epithelium, overexpressed in colorectal tumors (Hasegawa et al., 2013b; Tagi et al., 2010; Toulza et al., 2006).

The different expression patterns and cellular locations of DMKN isoforms suggest that their biological roles might differ. Insight into these putative functions appeared only very recently. We have previously shown that the ubiquitous and intracellular DMKN δ binds to and activates the small GTPase Rab5, revealing its involvement in early endosomal trafficking (Leclerc et al., 2011). A characteristic of the secreted DMKN β and γ is the presence of a central serine- and glycine-rich domain. The interaction between a 15-amino-acid peptide derived from this domain and a bacterial surface protein expressed by *Staphylococcus aureus*, the clumping factor B (ClfB), has been demonstrated by surface plasmon resonance assay. This suggests that DMKN β and γ could take part in the pathogenesis of this bacteria (Xiang et al., 2012). In another study, experiments using cultured normal human epidermal keratinocytes revealed that exogenous DMKN β inhibited phosphorylation of

Journal of Cell Science

Journal of Cell Science (2014) 127, 2862–2872 doi:10.1242/jcs.144808

extracellular-signal-regulated (ERK)1/2 and increased the expression of involucrin (IVL), suggesting that DMKN β is involved in keratinocyte differentiation through regulation of the ERK signaling pathway (Higashi et al., 2012). More recently, a putative role of Dmkn β during mouse skin wound healing has been reported. Topical treatments of injured mice with recombinant Dmkn β or its C-terminus domain delayed early stages of skin wound healing. This effect could have resulted from the modulation of chemokine expression (Hasegawa et al., 2013; Hasegawa et al., 2013a).

The murine *Dmkn* gene is conserved and located in the syntenic region of chromosome 7. The mouse SSC locus displays the same genomic organization as that of humans, with *Sbsn* and *Krtdap* flanking *Dmkn*, in the same orientation. *Dmkn* spans 22 exons and transcripts belonging to the α, β and γ isoforms have been described, but no messengers coding putative δ isoforms (Matsui et al., 2004; Moffatt et al., 2004; Naso et al., 2007). Here, we performed an in-depth characterization of the *Dmkn* transcripts expressed in the mouse skin. Using mice inactivated for Dmkn β and γ, we show for the first time that the corresponding isoforms play a role in epidermis terminal differentiation. Their absence leads to overexpression of Dmkn α and transient cornification defects.

RESULTS

Exhaustive analysis of the different *Dmkn* mRNAs and expression of the three SSC locus genes in mouse skin

We performed exhaustive RT-PCR experiments specifically designed to identify the α, β and γ isoform families using RNA extracted from newborn C57/Bl6 mouse epidermis. The sequences of some of the obtained amplicons strictly matched the mRNAs already described in the literature or public databases. We also identified three new splice variants, encoding one Dmkn β and two Dmkn γ isoforms, resulting from the alternative splicing of exon 6 and/or exon 9 (Fig. 1A). The small size of these alternative exons, encoding 15 and 16 amino acid residues, respectively, did not allow discrimination of the corresponding Dmkn β or γ isoforms by western blot analysis (data not shown). The presence of putative mRNAs encoding Dmkn δ isoforms was investigated by RACE-PCR. This did not allow the identification of messengers coding for these intracellular isoforms. In agreement with this result, we did not find any exon bearing a transcriptional start site specific to any δ isoforms by *in silico* analysis. In conclusion, expression of *Dmkn* in the skin is less complex in mouse than in human, and there is probably no expression of Dmkn δ transcripts.

During epidermal morphogenesis, the SSC locus genes show a coordinate spatio-temporal pattern of expression. It begins in the nasal epithelium at E14.5, simultaneously with the expression of other epidermal markers and the initiation of barrier formation (Bazzi et al., 2007). At birth, all the three genes are expressed in the whole skin. It is not known whether the expression is maintained later on. We thus compared, by quantitative RT-PCR, the expression of the SSC locus genes in the skin from newborn mice, and from young and old adult mice. As shown in Fig. 1B, a tendency towards increased expression of all the SSC locus genes, including their different splice variants, except for Dmkn γ, was observed with age. Statistically significant thresholds were found for transcripts encoding Dmkn α, Sbsn1, Sbsn2 and Krtdap1. These results suggest that proteins encoded by the SSC locus genes are necessary in the epidermis throughout life.

Expression of murine Dmkn during cutaneous wound healing

Dmkn gene expression starts concomitantly to the establishment of the epidermal barrier. We performed a kinetic analysis of *Dmkn* regulation when the barrier is challenged. This study focused on Dmkn β and γ, which are, contrary to Dmkn α, highly and specifically expressed by differentiated keratinocytes. Moreover, we successfully produced reliable antibodies recognizing these two isoforms, whereas antibodies specific to Dmkn α are not available. We created acute wounds on adult mouse dorsal skin and assessed Dmkn β and γ expression by immunohistochemistry during subsequent healing, from day 3 to day 10. The keratin K6, whose presence indicates a hyperproliferative state in parakeratotic keratinocytes, shows a strong labeling in early stages of wound healing, at day 3–5 (Fig. 1C). Dmkn β and γ labeling was also increased at day 3 post-wounding but remained at a high level in later stages of re-epithelialization. This seemed to correlate with return to an orthokeratotic differentiation pattern, when K6 was no longer expressed. From day 3 post-wounding, the increased labeling for Dmkn β and γ seemed to correlate with expression by an increased number of cell layers rather than an increased expression by individual cells. This expression pattern was similar to that of Ivl (Fig. 1C,D). Moreover, Dmkn β and γ labeling was concentrated at the apical pole of the cells (Fig. 1D). The same wave-like pattern, consistent with the localization of these Dmkn isoforms in lamellar bodies before secretion, was described in lesional skin of psoriatic patients (Toulza et al., 2006).

Deficiency of Dmkn β and γ does not affect barrier establishment or wound healing in mice

To investigate the role of Dmkn *in vivo*, we generated knockout (KO) mice, using the Cre-loxP system. We felt that the invalidation of the whole *Dmkn* gene was technically hazardous because of the very large size of the genomic DNA fragment necessary to excise. We thus chose to excise a smaller genomic region encompassing exon 1 to 5 (Fig. 2A,B). This strategy led to mice deficient in Dmkn β and γ [hereafter Dmkn $(\beta/\gamma)^{-/-}$ mice] but still able to express Dmkn α. Mice heterozygous for the Dmkn β and γ inactivation were phenotypically indistinguishable from their wild-type littermates. In homozygous Dmkn $(\beta/\gamma)^{-/-}$ mice, total absence of both Dmkn isoforms was verified by RT-PCR (data not shown) and immunohistochemistry (Fig. 2C). These mice were viable and fertile. Crossing of heterozygous parents produced all genotypes in the expected Mendelian ratio.

Because the *Dmkn* gene is expressed during epidermal embryonic morphogenesis, at the beginning of stratification, we analyzed the kinetics of epidermal barrier development *in utero*. However, the results of the dye penetration assays we performed on E17.5 embryos showed no differences between wild-type and KO animals (supplementary material Fig. S1A). We also analyzed whether Dmkn β and γ deficiency had an effect on wound healing after skin injury. Full-thickness wounds were performed on the flank of adult wild-type and KO mice and the kinetics of wound closure was monitored from day 0 to day 10 post-wounding (supplementary material Fig. S1B). The kinetics of wound closure could not be distinguished between wild-type and KO mice (supplementary material Fig. S1C). Finally, immunohistochemical labeling of skin wounds at day 3 and day 5 post-wounding revealed an infiltration of F4/80-positive macrophages and CD3-positive T cells in the same proportions in wild-type and KO wounds (supplementary material Fig. S2).

Journal of Cell Science (2014) 127, 2862–2872 doi:10.1242/jcs.144808

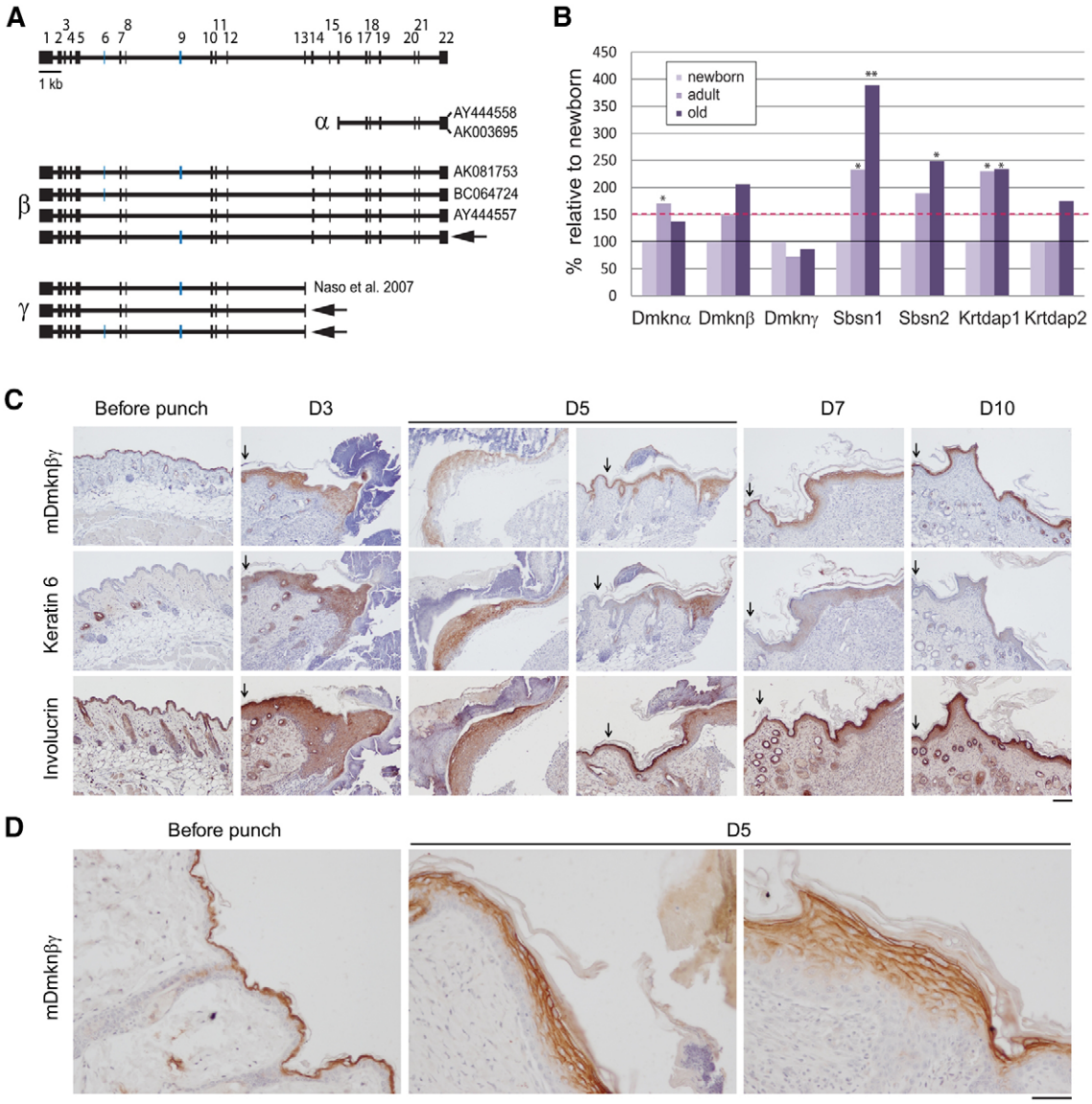

Fig. 1. Description of the *Dmkn* transcripts identified in mouse epidermis and analysis of the regulation of the murine SSC locus genes according to age. (A) Schematic representation of the murine *Dmkn* gene and its eight different transcripts. The three newly identified transcripts are indicated by arrows, exons by the black boxes and alternative exons 6 and 9 by the blue boxes. (B) Quantitative RT-PCR analysis of the expression of the SSC locus according to mouse age. Total RNAs were prepared from the skin of newborns (n=7), 8–10-week-old (adult, n=7) and 12-month-old (old, n=5) mice. The relative expressions of the SSC locus genes as compared to the newborn are shown. *P<0.5, **P<0.1. (C,D) Dmkn β and γ expression in the course of wound healing. Sections of unwounded and healing skin at day 3, 5, 7 and 10 post-wounding were processed for immunohistochemistry with anti-Dmkn-β/γ, anti-keratin-6 and anti-Ivl antibodies, as indicated. Arrows, edge of the original injury. Scale bars: 100 μm (C), 20 μm (D).

Overexpression of the SSC locus genes, including Dmkn α, and other late differentiation expressed genes in Dmkn $(\beta/\gamma)^{-/-}$ mice

We analyzed whether the absence of Dmkn β and γ modified the expression of either the other genes of the SSC locus or other late differentiation genes. This was investigated by quantitative RT-PCR performed on total RNA prepared from the skin of 3-day-old (P3) neonates. A striking feature was the strong overexpression (an eightfold increase) of transcripts encoding Dmkn α in the KO neonate epidermis in comparison to the wild-type littermate epidermis. Expression of transcripts encoding Sbsn1, Sbsn2 and Krtdap1 was also significantly increased, although to a lesser extent, with a ratio between KO and wild-type skin expression of 2.4, 2 and 2.1, respectively, whereas the levels of transcripts encoding Krtdap2 was unchanged (Fig. 3A). In mouse, the Dmkn α and β transcripts have been shown to be specifically expressed in various stratified epithelia, with the highest expression level in cornified epithelia, such as the epidermis, the epithelium of the tongue or the esophagus (Matsui et al., 2004). We thus analyzed, by quantitative RT-PCR, whether transcripts encoding Dmkn α were also overexpressed in such epithelia in the KO mice. Total mRNA was extracted from the skin of the ear, the tongue and the bladder of 15-day-old wild-type and KO mice. As shown in Fig. 3B, transcripts encoding Dmkn α were not expressed in the bladder, whereas its expression, when compared to wild-type,

Journal of Cell Science (2014) 127, 2862–2872 doi:10.1242/jcs.144808

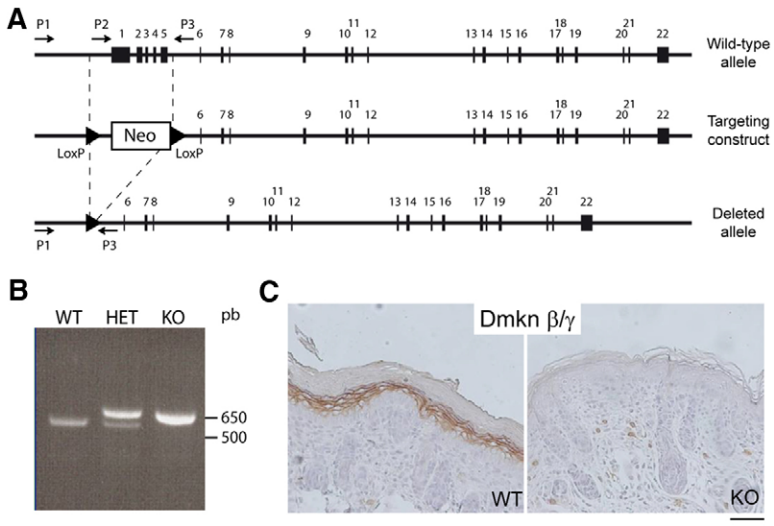

Fig. 2. *Dmkn* gene targeting. (A) Schematic drawing of the *Dmkn* wild-type locus, the targeting construct containing the neomycin selector gene, and the deleted allele obtained after Cre-mediated excision. Black boxes represent exons and black triangles loxP sites. Primers for PCR genotyping (P1–P3, listed in supplementary material Table S1) are indicated by arrows. (B) PCR analysis using primers P1, P2 and P3 of genomic DNA of the indicated genotypes. Primers P2 and P3 allow amplification of a 554-bp fragment from the wild-type (WT) allele, whereas primers P1 and P3 allow amplification of a 682-bp fragment from the knockout (KO) allele. (C) Immunohistochemical analysis using anti-Dmkn-β/γ antibody of newborn mouse dorsal skin showing expression of Dmkn β and γ in the granular layer of the epidermis of WT mice and absence of Dmkn β and γ in KO mice epidermis. Scale bar: 20 μm.

was increased by more than threefold in the skin and by more than twofold in the tongue of KO mice. These results suggest that, in Dmkn $(\beta/\gamma)^{-/-}$ mice, the expression of Dmkn α is increased not only in the skin but also in other epithelia normally expressing the *Dmkn* gene. We also detected a more than twofold increased expression of *Cdsn* and *Dsg1a* in KO neonates in comparison to the wild-type littermates, whereas the levels of *Flg* and *Ivl* showed no significant variations (Fig. 3C). It has previously been shown that DMKN β decreases the phosphorylation of ERK1/2 and subsequently increases caspase activity in cultured human keratinocytes (Higashi et al., 2012). Our analysis of the phosphorylation level of ERK1/2 by immunoblotting (Fig. 3D), as well as caspase-3 activation by immunohistochemistry (data not shown), did not show any modifications in KO compared to wild-type animal epidermis. Thus, we found evidence for a strong overexpression of Dmkn α at the mRNA level in Dmkn $(\beta/\gamma)^{-/-}$ mice, with no disruption of the signaling pathway in which Dmkn β and γ have been suggested to be involved.

Dmkn $(\beta/\gamma)^{-/-}$ mice develop a transient alteration of cornification

Although we did not find any obvious phenotypes in mice in the absence of Dmkn β and γ, a very careful examination of young pups revealed that KO mice developed a scaly skin during the first week of life (Fig. 4A). This phenotype was never observed in wild-type and heterozygous pups, and was no longer visible in KO mice by day 7–8, after hair growth occurred. At P3, examination of dorsal skin sections stained with hematoxylin and eosin revealed a reduced amount of keratohyalin granules in the *stratum granulosum* of KO mice in comparison to wild-type littermates (Fig. 4B). This was no longer visible in mice older than 8–10 days (data not shown). Ultrastructural examination of the KO mice skin confirmed these observations. The keratohyalin granules were also smaller. In addition, the lower *stratum corneum* of KO epidermis appeared more compact (Fig. 4C). We then analyzed the epidermal barrier of wild-type and KO pups (Fig. 5). Given that the cornified envelopes play an important role in the mechanical resistance and integrity of the *stratum corneum*, we first analyzed these structures isolated from mouse skin. Despite their similar morphology and comparable proportion of fragile and rigid envelopes (Fig. 5A), cornified envelopes isolated from KO newborns were more rapidly destroyed by sonication than wild-type ones. Only 10% remained intact after a 3-min sonication compared to 50% of wild-type cornified envelopes (Fig. 5B). We next asked whether this weakening of the cornified envelopes was accompanied by an alteration of the epidermal permeability. The inside-out permeability barrier was evaluated by measurement of the amount of water that was lost through the skin surface, the so-called trans-epidermal water loss (TEWL), and the outside-in permeability barrier was examined by Lucifer Yellow penetration assays. We found no difference between wild-type and KO pups at P5 (Fig. 5C,D). This demonstrated that the epidermal permeability barrier, which was properly established *in utero* (supplementary material Fig. S1), was maintained after birth in the KO mice.

Dmkn $(\beta/\gamma)^{-/-}$ mice display an increased processing of (pro)Flg and peculiar post-translational modification of Ivl but no obvious modification in the activity of transglutaminases and *stratum corneum* proteases

In order to understand the underlying mechanisms responsible for the described phenotype, we first analyzed the expression and processing of (pro)Flg in wild-type and KO mice. In agreement with the histological and ultrastructural appearance of the keratohyalin granules in the KO mouse epidermis, the intensity of immunohistological staining produced by the anti-Flg antibody was lower, as compared to wild-type skin (Fig. 6A). This difference seemed restricted to Flg, given that the expression of six other keratinocyte differentiation-related proteins, including two cornified envelope precursors, Ivl and loricrin, analyzed by immunological staining, did not revealed any difference between wild-type and KO pups (supplementary material Fig. S3). Immunoblot analysis of skin extracts showed that there was a global reduced level of (pro)Flg with a marked deficiency in Flg monomers in KO mice (Fig. 6B). Degradation of Flg monomers is a major source of amino acids in the *stratum corneum* that are part of the natural moisturizing factor (NMF) (Rawlings and Harding, 2004). To determine whether the reduced level of Flg monomers reflected a change in NMF production, we quantified the amount of free amino acids in the *stratum corneum* of wild-type and KO newborns. Six successive tape strips from the dorsal skin of wild-type and KO pups were collected and used to quantify the Flg degradation products pyrrolidone carboxylic

Journal of Cell Science (2014) 127, 2862–2872 doi:10.1242/jcs.144808

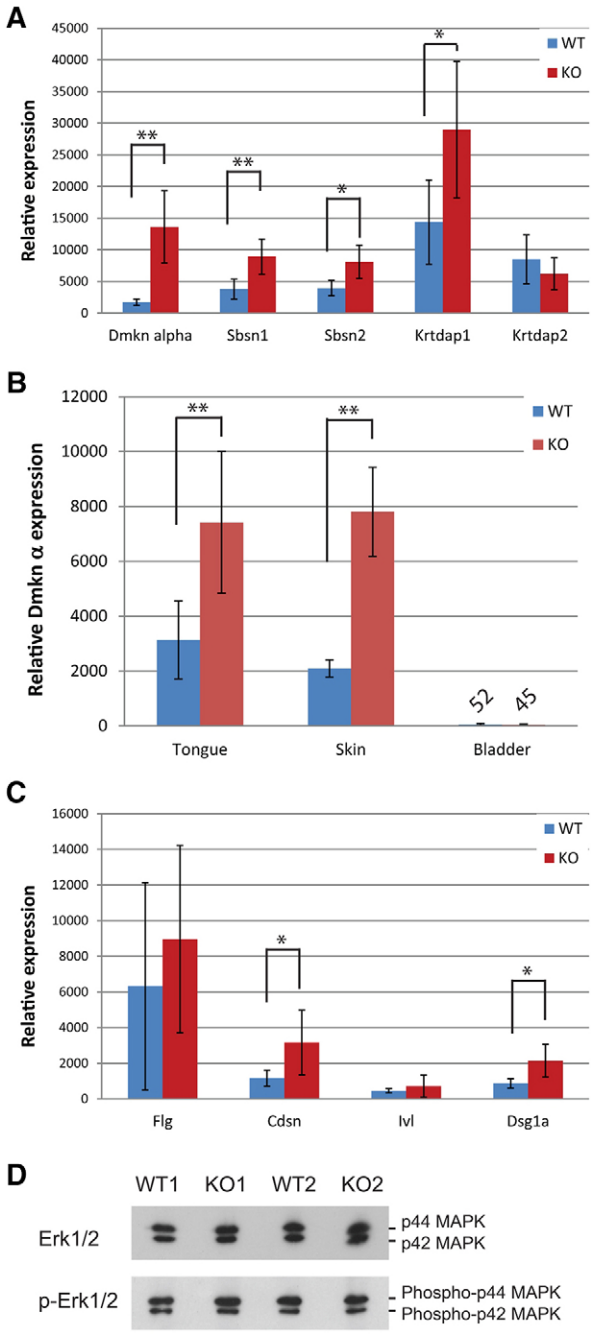

Fig. 3. Analysis of epidermal genes expression levels and signaling pathway involving Erk1/2 in Dmkn (β/γ)$^{-/-}$ mice. (A,B) Quantitative RT-PCR analysis of the expression of the SSC locus and epidermal differentiation genes. Total RNAs were prepared from the dorsal skin of wild-type (WT, $n=5$) or knockout (KO, $n=5$) pups (A,C) or from the skin of the ear, the tongue and the bladder of WT ($n=5$) or KO ($n=5$) 15-day-old mice (b). The expression relative to the the *Tbp* housekeeping gene of the SSC locus genes (A), of transcripts encoding Dmkn α (B) and of the differentiation genes *Flg*, *Cdsn*, *Ivl* and *Dsg1a* (C) are shown. *$P<0.05$, **$P<0.01$. (D) Immunoblot analysis of Erk1/2 and phosphorylated Erk1/2 (pErk1/2) expression in the skin of two WT and KO neonates. The detections were performed on the same membrane after dehybridization.

acid, cis- and trans-urocanic acid and histidine. The amount of NMF components present in the two more superficial strips showed a significant increase in KO mice compared to wild-type littermates (Fig. 6C). These results suggest that there is no defect in NMF production in KO mice but on the contrary an increased degradation of proFlg and Flg.

The scaly phenotype of the KO pups, as well as the more compact appearance of the lower *stratum corneum* of these mice, could be related to an alteration of cohesion or desquamation in the *stratum corneum*. Cohesion between corneocytes was investigated by quantification of proteins detached from the skin by tape-stripping. Six sequential tape strips were performed on the dorsal skin of wild-type and KO newborns. The amount of protein was unchanged in KO compared to wild-type pups, whether the comparison was realized between superficial (strips 1 and 2), intermediate (strips 3 and 4), deep (strips 5 and 6) or all (strips 1 to 6) collected corneocytes (Fig. 7A). The epidermal proteolytic activity was investigated by an *in situ* zymography assay. Again, no difference in the intensity of the fluorescence signal in the *stratum corneum*, reflecting the global activity of proteases, was highlighted between wild-type and KO epidermis (Fig. 7B).

Finally, we tried to clarify the molecular events responsible for the cornified envelope weakening. Transglutaminases are enzymes essential for the assembly of cornified envelopes in stratified squamous epithelia (Candi et al., 2005). Transglutaminase activity was compared in wild-type and KO epidermis by *in situ* enzymatic assay. The fluorescence signal resulting from the crosslinking of Alexa-Fluor®-555–Cadaverine at the cell periphery in the *stratum granulosum* was of similar intensity in both wild-type and KO epidermis (Fig. 8A). This suggests that there is no alteration in the function of enzymes responsible for cornified envelopes assembly in the KO pups. Ivl is one of the first proteins incorporated into the cornified envelope, besides envoplakin and periplakin. We found no difference in the expression of Ivl between wild-type and KO epidermis by qRT-PCR (Fig. 3C) and immunohistochemical staining (supplementary material Fig. S3). However, immunoblot analysis revealed a modification in the electrophoretic mobility of the protein (Fig. 8B). In accordance with previously published western blot analyses performed on skin extracts of C57Bl/6 mice, Ivl from wild-type mice ran as a major band of 56 kDa and a weaker 80-kDa band. This latter high-molecular-mass band might reflect transglutaminase crosslinking or lipid modification (Li et al., 2000). Both immunoreactive proteins were present in skin extracts of KO mice, but the 80-kDa band appeared weaker and an additional band of ~50 kDa was detected. This latter band cannot be explained by a different genetic background between wild-type and KO mice. Indeed, our KO mice were created in the 129 background but were repeatedly crossed (more than eight times) onto the C57Bl/6 background. Moreover, the *Ivl* and *Dmkn* genes reside on different chromosomes (chromosome 3 and 7, respectively). Thus we can presume that, in Dmkn (β/γ)$^{-/-}$ mice, the *Ivl* gene is on C57Bl/6 genetic background. In conclusion, our result suggests a different post-translational modification of Ivl in the KO mouse epidermis. Consistent with the transient phenotype, the additional 50-kDa band was not detected in skin extracts of adult KO mice (Fig. 8C).

DISCUSSION

In order to fully characterize the murine *Dmkn*, we performed an exhaustive analysis of its expression in the mouse epidermis by RT-PCR, RACE-PCR and *in silico* analysis. This confirmed that

Journal of Cell Science (2014) 127, 2862–2872 doi:10.1242/jcs.144808

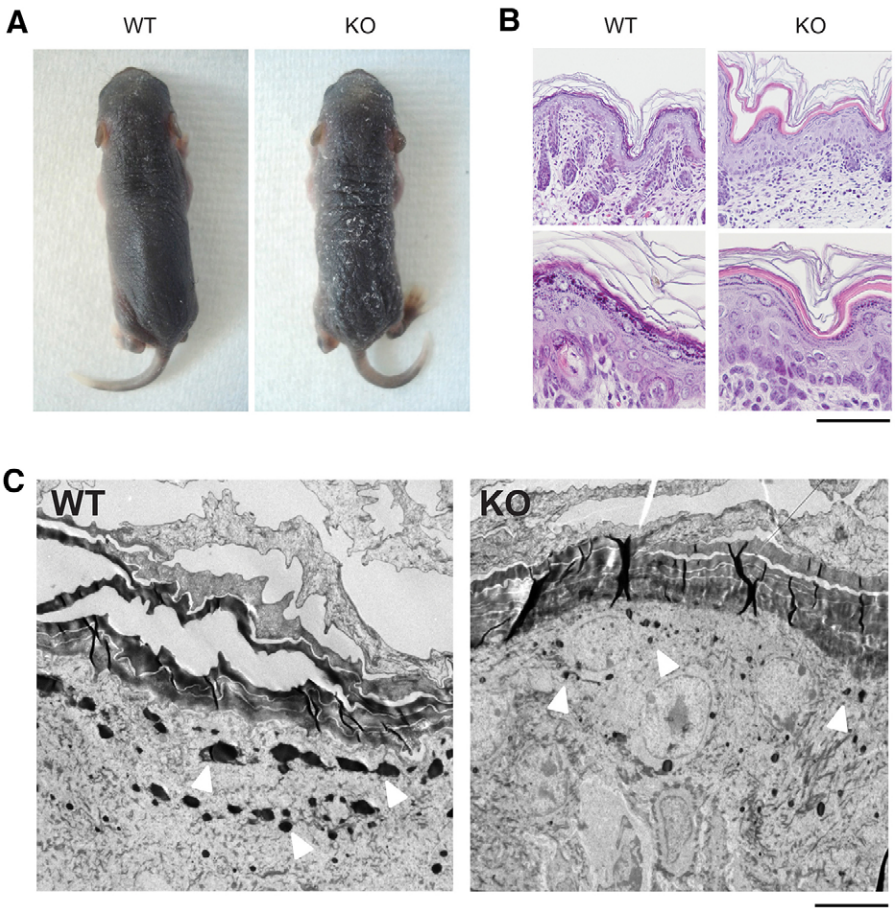

Fig. 4. Macroscopic, histological and ultrastructural phenotype of the Dmkn $(\beta/\gamma)^{-/-}$ mice. (A) Macroscopic appearance of wild-type (WT) and Dmkn $(\beta/\gamma)^{-/-}$ (KO) 5-day-old neonates. (B) Sections stained with hematoxylin and eosin from dorsal skin of WT and KO 3-day-old pups. (C) Ultrastructure of the dorsal skin of WT and KO 3-day-old pups. White arrowheads indicate smaller keratohyalin granules in the *stratum granulosum* of the KO newborns compared to WT ones. Scale bars: 20 μm (B, upper panel), 60 μm (B, lower panel), 5 μm (C).

Dmkn expression is less complex in mice than in humans. Including the three novel transcripts we identified, *Dmkn* encodes only four Dmkn β, three Dmkn γ and one Dmkn α isoform, whereas the complex Dmkn δ family of transcripts, described in humans, is absent in mouse. Moreover, our RT-PCR analysis suggests that *Dmkn* expression in mouse is coregulated with the two other SSC locus genes, *Sbsn* and *Krtdap*, according to age. All three genes, which encode secreted proteins still poorly characterized, could thus be related in their function during cornification.

In order to get more insight into the function of Dmkn β and γ, we produced mice deficient for these two isoforms. The Dmkn $(\beta/\gamma)^{-/-}$ mice were viable and fertile with no evident phenotype except a transient scaly skin during the first week of life. These proteins are thus dispensable during normal keratinocyte differentiation. A striking feature was the strong overexpression of transcripts encoding Dmkn α in the KO epidermis. Given the absence of reliable anti-Dmkn-α antibodies, this could not be confirmed at the protein level. This overexpression of transcripts encoding Dmkn α could result from the suppression, or the modification of the position, of some genomic regulatory sequences, caused by the excision of exons 1 to 5 of *Dmkn*. Another hypothesis is that it results from a compensatory mechanism. This is relevant given that the phenotype of scaly skin is temporary.

According to recently published data concerning overexpression of DMKN β in human keratinocytes, the absence of Dmkn β would be expected to lead to an increase in Erk phosphorylation resulting in a decrease in *Dmkn* and *Ivl* gene expression (Higashi et al., 2012). By contrast, our results show no difference in the balance between Erk and phosphorylated Erk in the skin of KO compared to control mice. This discrepancy might result from differences between humans and mice, or between *in vivo* and *in vitro* experiments.

In a recent work, Hasegawa et al. reported that Dmkn β and γ are induced during early stages of wound healing in mice (Hasegawa et al., 2013b). We confirmed the induced expression of these Dmkn at day 3 post-wounding. However, we noted that it persisted at later stages, until day 10. The same authors reported that topical application of recombinant Dmkn β or its C-terminal Glo2 domain inhibited mouse wound healing in early stages (day 2–3), but was without effect at later stages (day 5–12) (Hasegawa et al., 2013a). Although Dmkn α, which nearly corresponds to the C-terminal active Glo2 domain of Dmkn β, is overexpressed in our KO mice, absence of Dmkn β and γ had no impact on the kinetics of wound closure after acute skin injury. Further studies would be necessary to prove that the different murine Dmkn isoforms play a role during wound healing. Moreover, despite the strong and early expression of *Dmkn* during epidermal development *in utero* (Bazzi et al., 2007), absence of Dmkn β and γ had no effect on the kinetics of formation of the permeability barrier. In conclusion, although Dmkn β and γ are highly expressed in granular keratinocytes, our work suggests they are dispensable not only in normal epidermis but also during barrier establishment and wound healing in mice.

Journal of Cell Science (2014) 127, 2862–2872 doi:10.1242/jcs.144808

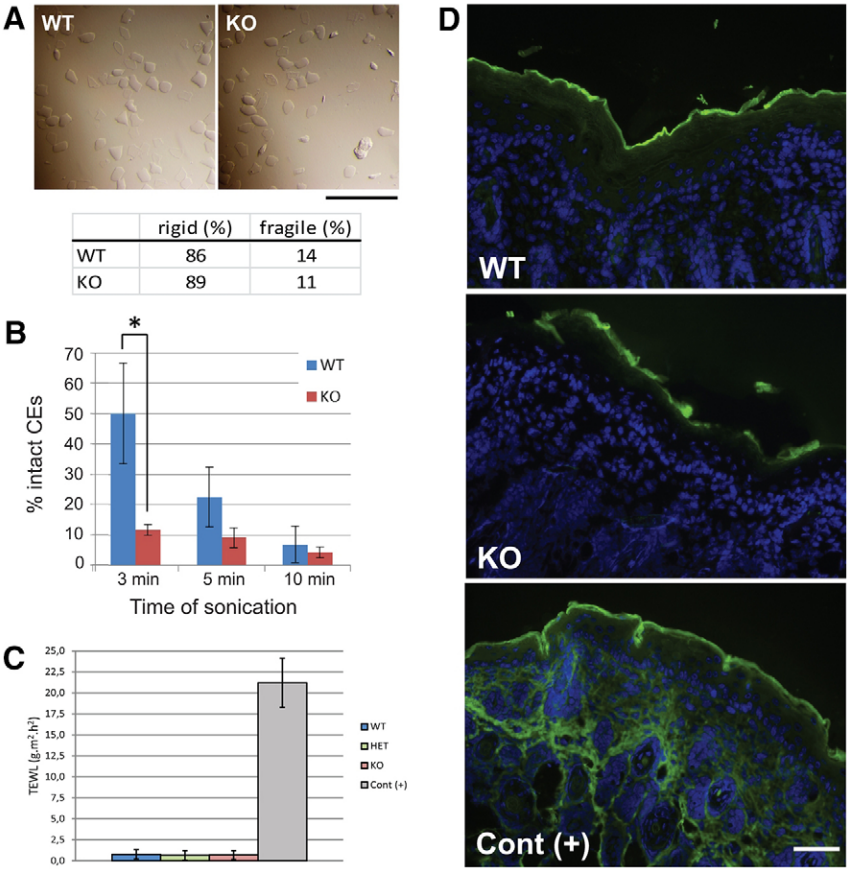

Fig. 5. Analysis of cornified envelopes mechanical resistance and skin barrier function in Dmkn $(\beta/\gamma)^{-/-}$ neonates. (A) Cornified envelopes purified from the skin of WT (n=3) and KO (n=3) neonates showed a similar morphology (upper panel) and proportion of rigid and fragile structures (lower panel). (B) Comparison of the resistance of cornified envelopes (CEs) from WT and KO mice after sonication. The percentage of intact envelopes relative to time 0 is reported for each time of sonication. *P<0.05. Values are mean±s.e.m. (C) TEWL measurements performed on the dorsal skin of WT (n=12), heterozygous (HET, n=18) and KO (n=14) 5-day-old pups. Positive control [Cont(+)] corresponds to TEWL measurement after ten successive tape strippings of the dorsal skin of WT pups (n=7). Values are mean±s.e.m. (D) Transdermal diffusion assay of the fluorescent dye Lucifer Yellow in dorsal skin explants from 5-day-old WT or KO pups. For the positive control [Cont(+)] the dorsal skin of a WT pup was subjected to ten sequential tape strippings before processing for the assay. Nuclei were counterstained with DAPI. Scale bars: 200 µm (A), 20 µm (D).

We highlighted a transient phenotype of scaly skin in the Dmkn $(\beta/\gamma)^{-/-}$ mice. This phenotype did not cause any disruption of the permeability barrier, as evaluated by penetration of external dye and TEWL measurements, and was visible only during the first week of life. Similar transitory phenotypes have been described in the case of mice deficient in loricrin (Koch et al., 2000) and mice deficient in Ivl, envoplakin and periplakin (Sevilla et al., 2007). This suggests that compensatory mechanisms can be rapidly established when the epidermal barrier is challenged.

This very transient nature of the phenotype probably contributes to difficulty in elucidating the underlying mechanisms. Indeed, the more compact appearance of the lower *stratum corneum* and the scales at the skin surface of the Dmkn $(\beta/\gamma)^{-/-}$ mice could be related to an increased cohesion between corneocytes and/or a reduced desquamation. However, we did not detect any defect in *stratum corneum* cohesion or protease activity in the KO epidermis.

KO pups contained smaller keratohyalin granules, and presented reduced levels of proFlg and Flg monomers as well as a significantly higher level of components of the NMF in the superficial *stratum corneum*. The downregulation of (pro)Flg very likely is mediated at the post-translational level, because we did not find any change in the *Flg* mRNA level in KO versus wild-type skin in 3-day-old neonates. This suggests that (pro)Flg processing is increased in the KO epidermis. A drastic decrease in proFlg, Flg-processing intermediates and Flg monomers was described in mice overexpressing elastase 2, a protease able to progressively degrade all forms of Flg *in vitro*, from the precursor to the monomer (Bonnart et al., 2010). Reduced levels or complete absence of Flg monomers have also been described in a number of other experimental mouse models (e.g. in mice null for Pig-a, CAP1/Prss8, caspase-14, matriptase/MT-SP1 or Flg mice), but it was linked to either a blockade in the processing of (pro)Flg or a total absence of proFlg synthesis (Denecker et al., 2007; Hara-Chikuma et al., 2004; Kawasaki et al., 2012; Leyvraz et al., 2005; List et al., 2003). By contrast, an accumulation of Flg monomers was described in the case of *Spink5*$^{R820X/R820X}$ mice and of mice overexpressing claudin 6 (Hewett et al., 2005; Turksen and Troy, 2002). In both cases, the accumulation was linked to an accelerated processing of proFlg into Flg monomers, but the consequence on NMF production or free amino acid content in the *stratum corneum* was not analyzed. In the present study, our hypothesis is that an accelerated (pro)Flg processing and an increased level of NMF compounds occur soon after birth (under a dry environment) as a compensatory mechanism to the absence of Dmkn β and γ. Whether this increased production of NMF is responsible for maintaining a normal *stratum corneum* hydration and TEWL in the KO epidermis remains to be determined. Indeed, Flg is the main source of free amino acids and derivatives, and thus considered to play a crucial role in *stratum corneum* hydration. However, recent findings using *Flg*$^{-/-}$ mice, which exhibited a marked decrease in NMF values but normal TEWL and *stratum corneum* hydration, incite to carefully interpret the relations between Flg and hydration (Kawasaki et al., 2012).

Flg monomers are also components of the cornified envelope, and might constitute as much as 10% of total cross-linked cornified envelope protein (Steven and Steinert, 1994). Thus, we

Journal of Cell Science (2014) 127, 2862–2872 doi:10.1242/jcs.144808

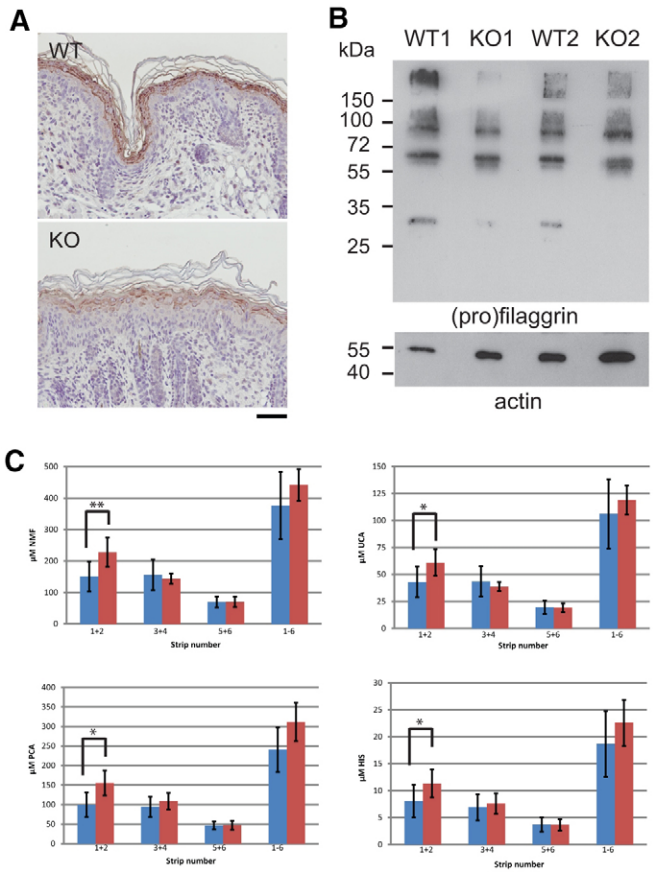

Fig. 6. Filaggrin expression, processing, and NMF production in wild-type and Dmkn (β/γ)$^{-/-}$ neonates. (A) Immunohistochemical staining with anti-filaggrin antibody of sections from dorsal skin of WT and KO 3-day-old pups. Scale bar: 20 µm. (B) Analysis of (pro)filaggrin expression in the epidermis of WT and KO mice by immunoblotting. Equal amount of protein extracts from two WT and two KO 3-day-old mice were separated by SDS-PAGE and subjected to immunoblotting with antibodies specific for (pro)Flg (upper panel) or actin (lower panel). The positions of molecular mass markers are indicated on the left. (C) Quantification of NMF components in the *stratum corneum* of 5-day-old pups. Tape stripping was performed on the dorsal skin of WT (n=7) and KO (n=7) pups. Tapes were pooled in pairs (1+2, 3+4 and 5+6) and used to quantify pyrrolidone carboxylic acid (PCA), cis- and trans-urocanic acid (UCA) and histidine (HIS) by high-performance liquid chromatography. Values from the more superficial (1+2), intermediate (3+4) and lower (5+6) strips are shown. NMF values correspond to the sum of PCA, trans-UCA, cis-UCA and HIS values. Values are mean±s.e.m. *P<0.05, **P<0.01.

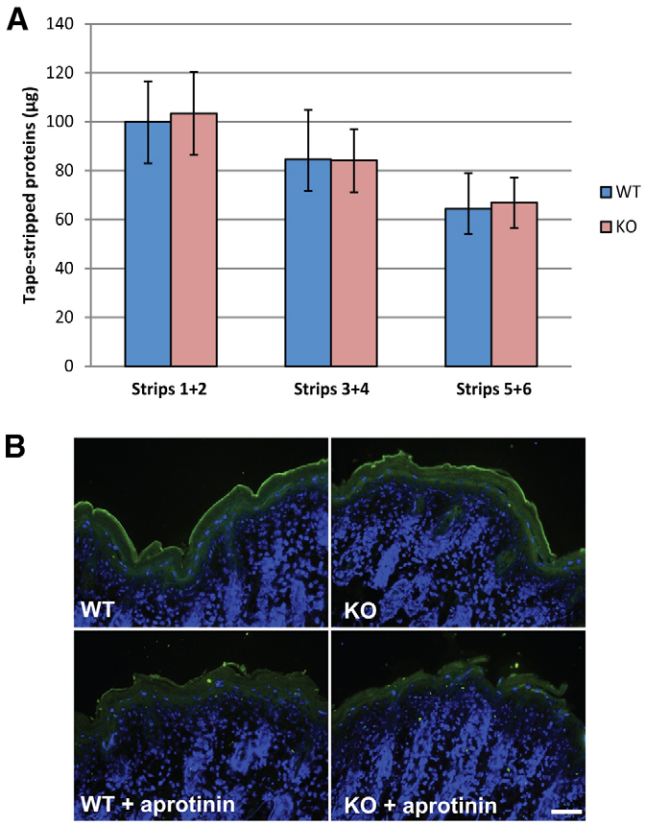

Fig. 7. Analysis of *stratum corneum* cohesion and desquamation in 5-day-old wild-type and Dmkn (β/γ)$^{-/-}$ mice. (A) Mechanical resistance assay of the *stratum corneum* from newborns. Tape stripping was performed on the dorsal skin of WT (n=5) or KO (n=5) pups, and the proteins present on the tape were quantified by colorimetric assay. Values from the more superficial (strips 1+2), intermediate (3+4) and lower (5+6) strips are shown. Values are mean±s.e.m. (B) Protease activity in the *stratum corneum* of WT and KO newborns was analyzed by *in situ* zymography. Green fluorescence indicates the proteolytically released BODIPY moiety, nuclei are counterstained with DAPI. A control reaction which includes the serine protease inhibitor, aprotinin, is shown. Scale bar: 20 µm.

cannot exclude the possibility that the reduced level of Flg monomers contributes to the cornified envelope weakening observed in the Dmkn (β/γ)$^{-/-}$ epidermis. Post-translational modification of Ivl was also obvious in KO pup epidermis, with the appearance of an additional lower molecular mass form of this cornified envelope precursor. Although Ivl has been extensively studied in the past, there are very few data about heterogeneity in its electrophoretic mobility and putative consequence on keratinocyte physiology. Such changes have been described in mice as inter-strain variation related to the number of tandem repeats of the protein (Delhomme and Djian, 2000). Second, for a given mouse strain, the electrophoretic mobility of Ivl extracted from cultured keratinocytes was different from that extracted directly from the epidermis (Li et al., 2000). This was hypothesized to reflect differences in transglutaminase crosslinking, lipid modification or proteolytic degradation, possibly linked to differences in early events of cornified envelope assembly. In the present study, the modifications of Ivl electrophoretic mobility suggest that absence of Dmkn β and γ can modulate, directly or indirectly, the processing of this cornified envelope precursor, and could explain the weakening of the cornified envelopes observed in the KO pup epidermis. The smaller size form of Ivl in the epidermis of KO pups could correspond to a proteolytic cleavage. *In silico* analysis reveals many cleavage sites recognized by different protease families in Ivl (data not shown). Further analysis are necessary to determine the potential cleavage sites, the protease(s) involved and the impact of this post-translational modification on cornification.

Overall, this study brings new data on the characterization and expression of *Dmkn* and, more globally, SSC locus genes, in mice. It is the first report evidencing for a role of Dmkn β/γ in keratinocyte terminal differentiation. The underlying molecular events linking Dmkn β/γ and cornification remain to be identified.

Journal of Cell Science (2014) 127, 2862–2872 doi:10.1242/jcs.144808

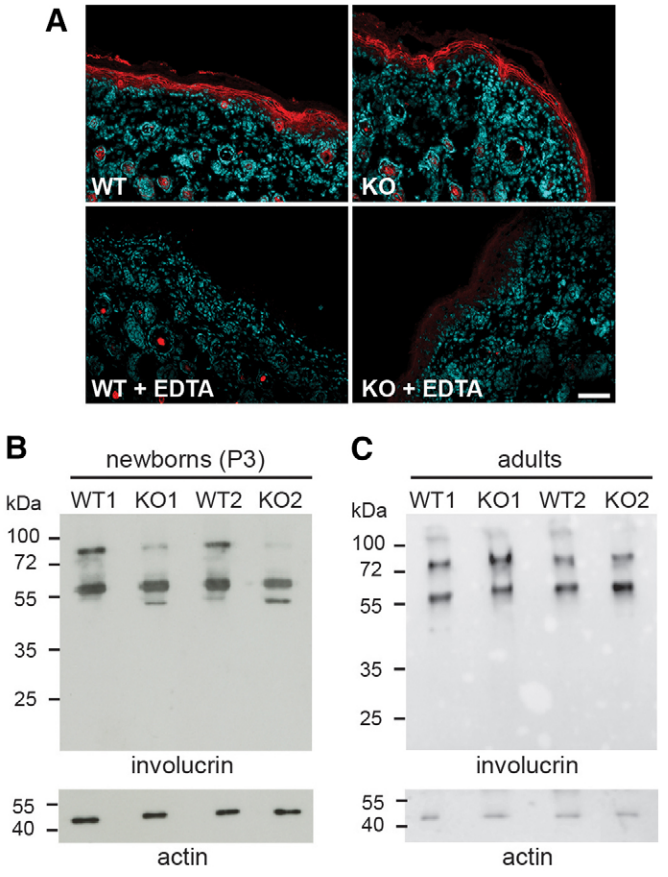

Fig. 8. Analysis of transglutaminase activity and involucrin expression in wild-type and Dmkn (β/γ)$^{-/-}$ mice. (A) An *in situ* transglutaminase activity assay was performed on skin cryosections from WT or KO 5-day-old newborns. Red fluorescence indicates the pericellular crosslink of Alexa-Fluor-555–Cadaverine in the *stratum granulosum* of both WT and KO epidermis with similar intensity. Nuclei are counterstained with DAPI. Scale bar: 20 µm. (B,C) Analysis of Ivl expression in WT and KO mice by immunoblotting. Equal amounts of protein extract from two WT and two KO 3-day-old (B) and adult (C) mice were separated by SDS-PAGE and subjected to immunoblotting with antibodies specific for Ivl (upper panel) or actin (lower panel). The position of molecular mass markers are indicated on the left.

MATERIALS AND METHODS

Generation of mice and animal protocols

Animals were handled according to the institutional guidelines and policies. The *Dmkn* mutant mouse line was established at the MCI/ICS (Mouse Clinical Institute/Institut Clinique de la Souris, Illkirch, France). The targeting vector was constructed as follows. The 5′ arm (3.7 kb) and 3′ (3.4 kb) homology arms were amplified by PCR (from 129S2/SvPas genomic DNA) and sequentially subcloned in a MCI proprietary vector containing a floxed Neo cassette. All the coding regions were sequenced. The linearized construct was electroporated in 129S2/SvPas mouse embryonic stem cells (ESCs). After G418 selection, targeted clones were identified by PCR using external primers and further confirmed by Southern blotting with both Neo 5′ and 3′ external probes. One positive ESC was injected into C57BL/6J blastocysts, and derived male chimeras gave germline transmission. Chimeric offspring were mated with a Cre deleter female that expresses the Cre recombinase to excise the neomycin selection marker flanked by LoxP sites. The Cre transgene was segregated in a supplementary breeding step.

For wound healing experiments, the dorsal hair of 8–10-week-old male mice was shaved 24 h before wounding. Mice were anesthetized intraperitoneally and full-thickness wounds (four per mouse) were performed using a 6-mm biopsy punch (Miltex, Ratingen, Germany). For analysis of the expression of Dmkn β/γ in the course of wound healing, five C57Bl/6 mice were killed 3, 5, 7 or 10 days post-wounding and wounds were harvested and processed for histological or immunohistological analysis. For the analysis of the kinetic of wound closure in wild-type versus KO mice, five wild-type and five KO mice were used for each time point (3, 5, 7 or 10 days). Wounds were photographed with a digital camera (Sony DSC-W50) and the wound area was calculated using ImageJ software.

RNA isolation, reverse transcription, RACE-PCR and quantitative real-time PCR

RACE PCR was performed as follows. Frozen new-born skin of C57BL/6 mice were incubated, epidermis side up, for 1 h at 4°C in phosphate-buffer saline (PBS) containing 0.5 mg/ml thermolysin (T7902, Sigma, St Louis, MO). The epidermis was removed with forceps and RNA was extracted according the Qiagen RNA easy mini kit procedure (Qiagen, Hilden, Germany). We performed 5′ RNA ligase-mediated (RLM)-RACE using the FirstChoice RLM-RACE kit (Ambion, Austin, TX) as described previously (Toulza et al., 2007). Briefly, total RNA was dephosphorylated with calf intestine phosphatase then decapped using tobacco acid pyrophosphatase to target full-length mRNA. An adapter was then ligated to mRNA, and reverse transcription was performed using an oligo(dT) primer. PCR was performed to amplify the cDNA using the outer 5′ RLM-RACE and the lower primer (5′-CTCCC-ACAGTTTGCGGAAGT-3′). Nested PCR was then performed with the inner 5′ RLM-RACE primer. The RACE nested PCR products were cloned into a pCRII-TOPO vector using a TOPOT/A cloning kit (Life Technologies, Paisley, UK) and sequenced.

For quantitative RT-PCR experiments, RNAs were isolated according to the RNeasy mini columns protocol (Qiagen, Hilden, Germany) from skin samples frozen immediately after dissection. Reverse transcription was performed using an oligo(dT) primer. Primer sequences (supplementary material Table S2) were designed using Primer3 software to generate amplicons of 100–250 bp encompassing different exons. BLAST analysis (Altschul et al., 1997) ensured the absence of similarity to any other mouse sequence. Amplification assays were performed with the 7300 Real Time PCR System using the Sybr qPCR SuperMix with ROX (Life Technologies, Paisley, UK). Fluorescence was quantified as Ct (threshold cycle) values. Samples were analyzed in triplicate, with differences between the three Ct values lower than 0.3. Relative levels of gene expression between samples were determined using *Tbp* expression for normalization. Control wells (without template cDNA) emitted no significant fluorescence. Specificity was assessed by sequencing the qRT-PCR amplicons.

Primary antibodies

Commercially available antibodies used in the study are listed in supplementary material Table S3. Anti-peptide antibody directed against Dmkn β/γ was produced by rabbit immunization with two synthetic peptides conjugated, through an added N- or C-terminal cysteine residue, to keyhole-limpet hemocyanin (Genosphere, Paris, France). The peptides were synthesized according to the predicted amino acid sequence of mouse Dmkn β/γ (A^{33}SAAHGAGDAISHG^{46} and D^{85}VFEHRLGEAARSL^{97}). The antiserum was affinity-purified on the recombinant mouse Dmkn γ coupled to an agarose-activated affinity column (AminoLink™ kit, Pierce Biotechnology, Rockford, IL). Mouse monoclonal antibody F28-27, raised against human CDSN, which cross reacts with mouse Cdsn, was used as previously described (Leclerc et al., 2009).

Histological, immunohistological and transmission electron microscopy experiments

Mouse skin samples were fixed for 24 h in 4% formalin, and were then paraffin embedded. Sections (5 µm) were stained with hematoxylin and eosin or processed for immunohistochemical analysis. The dilution of the primary antibodies is listed in supplementary material Table S3. The rabbit anti-Dmkn β/γ was diluted 1:500. In the case of immunodetection with anti-active caspase-3 and anti-Dmkn-β/γ antibodies, heat-induced epitope retrieval was performed by incubation of the sections for 40 min

at 95℃ in 50 mM glycine-HCl pH 3.5. Rabbit polyclonal antibodies were detected with the ImmPRESS anti-rabbit Ig (peroxidase) kit (Vector Laboratories, Burlingame, CA). For immunofluorescence, Alexa-Fluor®-555-conjugated goat anti-mouse IgG (Life Technologies, Paisley, UK) was diluted 1:1000 and used for detection of primary mouse antibodies. Images were taken using a Nikon eclipse 80i microscope equipped with a Nikon DXM 1200C digital camera and NIS image analysis software. For transmission electron microscopy, samples were prepared exactly as previously described (Leclerc et al., 2009), and ultrathin sections were examined with an electron microscope (H7700 Hitachi).

Protein extraction, SDS-PAGE and western blot analysis

Dermo-epidermal cleavage of newborn mouse skin was performed by heat treatment and the epidermis was extracted as previously described (Leclerc et al., 2009). Briefly, the epidermis was homogenized in extraction buffer (40 mM Tris-HCl pH 7.4, 10 mM EDTA, 8 M urea, 0.25 mM PMSF) with 1% v/v protease inhibitor cocktail and 1% phosphatase inhibitor cocktail (Sigma, St Louis, MO) using the FastPrep homogenizer (MP Biomedicals, Santa Ana, CA). Equal quantities of protein were separated by 12.5% SDS-PAGE and transferred to nitrocellulose membrane. The blots were probed with commercially available primary antibodies diluted as recommended by the manufacturer (supplementary material Table S3) then with horseradish peroxidase (HRP)-conjugated secondary antibody (Life Technologies, Paisley, UK). Detection was performed with ECL or ECL-Prime reagent (GE Healthcare, Uppsala, Sweden).

Skin barrier function assays

Development of epidermal barrier *in utero* was analyzed by a dye penetration assay, essentially as described by Hardman et al. (Hardman et al., 1998). The developmental stage of mouse embryos was determined based on the assumption that fertilization occurred in the middle of the dark cycle the day before plugs were identified. The embryos were dehydrated by series of 1-min incubations in 25%, 50% and 75% methanol in PBS and 100% methanol, then rehydrated for 3 min in PBS and stained for 1 min in 0.0125% toluidine blue in PBS. After destaining in PBS, embryos were photographed with a digital camera (Sony DSC-W50). The step of development of the permeability barrier was established by three independent blind classifications of stained embryos according to the gradual levels (from stage i to viii) previously proposed (Hardman et al., 1998).

TEWL was measured using a tewameter TM 300 (Courage & Khazaka electronic, Cologne, Germany). For transdermal absorption of fluorescent dye, newborn mice were killed, their dorsal skin was removed and spread on a gauze soaked with PBS in a Petri dish. Using a cloning cylinder, 100 µl of 0.4 mg/ml of Lucifer Yellow (Sigma) was put into contact with the skin. After 1 h of incubation at 37℃, the skin was frozen. Cryosections (5 µm) were counterstained with 4′,6-diamidino-2-phenylindole (DAPI) and then analyzed by fluorescence microscopy.

For some experiments, sequential tape stripping was performed. A D-Squame disc (14-mm diameter, Monaderm, Monaco) was attached to the dorsal skin of 5-day-old pups, pressed for 10 s and stripped off. The process was repeated five times on the same area and stored in a closed vial at −20℃ until analysis. The amount of protein per D-Squame disc was measured as previously described (Leclerc et al., 2009). Briefly, tape disc fragments were incubated with shaking in extraction buffer (40 mM Tris-HCl pH 7.4, 10 mM EDTA, 8 M urea, 50 mM dithiothreitol, 0.25 mM PMSF) for 2 h at 70℃, then centrifuged for 5 min at 13000 ***g*** and the protein content was measured in the supernatant using the Bradford colorimetric protein assay (Bio-Rad, Hercules, CA).

NMF dosage from tape-stripping of mouse skin

The concentrations of pyrrolidone carboxylic acid, cis-, trans-urocanic acid and histidine were determined as described previously (Dapic et al., 2013). Briefly, the tape strips were extracted by using 25% ammonia solution. Ammonia extracts were evaporated to dryness using an Eppendorf Concentrator 5301 device (Eppendorf AG, Hamburg, Germany). To each sample, 500 µl water was added and subsequently analyzed by HPLC 250 using a 3-mm reversed-phase Synergi 4-mm Polar-RP 80A column (Phenomenex, Torrance, CA).

Isolation and analysis of cornified envelopes

Newborn mouse skin (~0.5 cm^2) was boiled for 10 min at 95℃ under vigorous agitation in cornified envelope isolation buffer (100 mM Tris-HCl pH 8.5, 20 mM DTT, 5 mM EDTA) containing 2% SDS. Cornified envelopes were centrifuged at 12,000 ***g*** and resuspended in cornified envelope isolation buffer containing 2% SDS. This extraction procedure was repeated four times, with an incubation time at 95℃ extended to 1 h during the last extraction. Purified cornified envelopes were then washed three times in isolation buffer containing 0.2% SDS and conserved at +4℃ in the same buffer. Images of cornified envelopes were taken by phase-contrast microscopy using a Nikon eclipse 80i microscope equipped with a Nikon DXM 1200C digital camera and NIS image analysis software. The proportion of fragile versus rigid cornified envelopes was determined by counting an average of 1400 cornified envelopes for each sample of purified cornified envelope ($n=6$). For sonication experiments, the cornified envelope suspension (2×10^5 per ml) was sonicated in a Misonix 4000 MPX sonicator equipped with a cup horn for 1 to 10 min (60% amplitude). Intact cornified envelopes were then double-blind counted using a hemocytometer. Experiments were performed on cornified envelopes isolated from three newborn mice per genotype, samples were analyzed in duplicates and the experiment was repeated once.

In situ enzymatic assays

For detection of protease activity in the skin of mouse skin, frozen sections (5 µm) were rinsed with 1% Tween-20 in desionized water and incubated at 37℃ for 2 h with 2 µg/ml BODIPY®-FL-casein in 10 mM Tris-HCl, pH 7.8 (Molecular probes, Eugene, OR). After removal of excess of substrate solution, nuclei were stained with DAPI. In some experiments, 20 µg/ml aprotinin (Sigma, St Louis, MO) was added to inhibit serine protease activity. *In situ* transglutaminase activity assay was performed as described previously (Raghunath et al., 1998). In brief, 5-µm cryosections were blocked with 1% BSA in 0.1 M Tris-HCl pH 8.4 for 30 min and then incubated for 1 h at room temperature with 50 µM Alexa-Fluor®-555–cadaverine (Life Technologies, Paisley, UK) in 0.1 M Tris-HCl pH 8.4 containing DAPI and either 5 mM $CaCl_2$ or 25 mM EDTA (negative control). The reaction was stopped by incubating the sections with 25 mM EDTA in PBS for 5 min then sections were rinsed with PBS and mounted. Assays were visualized with a Zeiss axio observer z1 inverted microscope or a Nikon eclipse 80i microscope.

Acknowledgements

The *Dmkn* mutant mouse line was established at the Mouse Clinical Institute (MCI/ICS). We thank Sabrina Benaouadi, Emilie Amblard and Géraldine Gasc for excellent technical assistance. We thank staff of INSERM-IFR150 and UMS 006, and more particularly Marilyne Calise, Sylvie Appolinaire, Aline Tridon and Patrick Aregui from the animal facilities, and Florence Capilla and Tala Al Saati from the technical platform of 'histopathologie expérimentale'. We thank Laure Buisson and Emilie Amblard from the 'plateau de séquençage' of UMR 5165 CNRS – 1056 INSERM, Bruno Payré from the CMEAB for ultrastructural analysis and Olivier Andreoletti from UMR INRA ENVT 1225 for sonication experiments. We wish to acknowledge Michel Simon from UMR5165/U1056 'Différenciation Epidermique et Autoimmunité Rhumatoïde' for critically reviewing the manuscript.

Competing interests

The authors declare no competing interests.

Author contributions

E.A.L. designed, performed and analyzed most of experiments. A.H. designed, performed and analyzed RACE-PCR experiments, took care of animal breeding and performed experiments on mice. S.K. performed experiments and analyzed data obtained concerning quantification of components of NMF. G.S. supervised the project and critically reviewed the manuscript. N.J. designed and performed experiments, analyzed data, supervised the project and wrote the manuscript with contribution from all the authors.

Funding
This study was supported by grants from the Centre national de la recherche scientifique (CNRS); Institut national de la santé et de la recherche médicale (INSERM); and Toulouse III University. E.A.L. was a recipient of the 2010 Greentech award.

Supplementary material
Supplementary material available online at
http://jcs.biologists.org/lookup/suppl/doi:10.1242/jcs.144808/-/DC1

References

Altschul, S. F., Madden, T. L., Schäffer, A. A., Zhang, J., Zhang, Z., Miller, W. and Lipman, D. J. (1997). Gapped BLAST and PSI-BLAST: a new generation of protein database search programs. *Nucleic Acids Res.* **25**, 3389-3402.

Bazzi, H., Fantauzzo, K. A., Richardson, G. D., Jahoda, C. A. and Christiano, A. M. (2007). Transcriptional profiling of developing mouse epidermis reveals novel patterns of coordinated gene expression. *Dev. Dyn.* **236**, 961-970.

Bonnart, C., Deraison, C., Lacroix, M., Uchida, Y., Besson, C., Robin, A., Briot, A., Gonthier, M., Lamant, L., Dubus, P. et al. (2010). Elastase 2 is expressed in human and mouse epidermis and impairs skin barrier function in Netherton syndrome through filaggrin and lipid misprocessing. *J. Clin. Invest.* **120**, 871-882.

Candi, E., Schmidt, R. and Melino, G. (2005). The cornified envelope: a model of cell death in the skin. *Nat. Rev. Mol. Cell Biol.* **6**, 328-340.

Dapic, I., Jakasa, I., Yau, N., Kezic, S. and Kammeyer, A. (2013). Evaluation of an HPLC method for the determination of natural moisturizing factors in the human stratum corneum. *Anal. Lett.* **46**, 2133-2144.

Denecker, G., Hoste, E., Gilbert, B., Hochepied, T., Ovaere, P., Lippens, S., Van den Broecke, C., Van Damme, P., D'Herde, K., Hachem, J. P. et al. (2007). Caspase-14 protects against epidermal UVB photodamage and water loss. *Nat. Cell Biol.* **9**, 666-674.

Delhomme, B. and Djian, P. Gene. (2000). Expansion of mouse involucrin by intra-allelic repeat addition. *Gene* **252**,195-207.

Hara-Chikuma, M., Takeda, J., Tarutani, M., Uchida, Y., Holleran, W. M., Endo, Y., Elias, P. M. and Inoue, S. (2004). Epidermal-specific defect of GPI anchor in Pig-a null mice results in Harlequin ichthyosis-like features. *J. Invest. Dermatol.* **123**, 464-469.

Hardman, M. J., Sisi, P., Banbury, D. N. and Byrne, C. (1998). Patterned acquisition of skin barrier function during development. *Development* **125**, 1541-1552.

Hasegawa, M., Higashi, K., Matsushita, T., Hamaguchi, Y., Saito, K., Fujimoto, M. and Takehara, K. (2013a). Dermokine inhibits ELR(+)CXC chemokine expression and delays early skin wound healing. *J. Dermatol. Sci.* **70**, 34-41.

Hasegawa, M., Higashi, K., Yokoyma, C., Yamamoto, F., Tachibana, T., Matsushita, T., Hamaguchi, Y., Saito, K., Fujimoto, M. and Takehara, K. (2013b). Altered expression of dermokine in skin disorders. *J. Eur. Acad. Dermatol. Venereol.* **27**, 867-875.

Hewett, D. R., Simons, A. L., Mangan, N. E., Jolin, H. E., Green, S. M., Fallon, P. G. and McKenzie, A. N. (2005). Lethal, neonatal ichthyosis with increased proteolytic processing of filaggrin in a mouse model of Netherton syndrome. *Hum. Mol. Genet.* **14**, 335-346.

Higashi, K., Hasegawa, M., Yokoyama, C., Tachibana, T., Mitsui, S. and Saito, K. (2012). Dermokine-β impairs ERK signaling through direct binding to GRP78. *FEBS Lett.* **586**, 2300-2305.

Kawasaki, H., Nagao, K., Kubo, A., Hata, T., Shimizu, A., Mizuno, H., Yamada, T. and Amagai, M. (2012). Altered stratum corneum barrier and enhanced percutaneous immune responses in filaggrin-null mice. *J. Allergy Clin Immunol* **129**, 1538-1546 e6.

Koch, P. J., de Viragh, P. A., Scharer, E., Bundman, D., Longley, M. A., Bickenbach, J., Kawachi, Y., Suga, Y., Zhou, Z., Huber, M. et al. (2000). Lessons from loricrin-deficient mice: compensatory mechanisms maintaining skin barrier function in the absence of a major cornified envelope protein. *J. Cell Biol.* **151**, 389-400.

Leclerc, E. A., Huchenq, A., Mattiuzzo, N. R., Metzger, D., Chambon, P., Ghyselinck, N. B., Serre, G., Jonca, N. and Guerrin, M. (2009). Corneodesmosin gene ablation induces lethal skin-barrier disruption and hair-follicle degeneration related to desmosome dysfunction. *J. Cell Sci.* **122**, 2699-2709.

Leclerc, E. A., Gazeilles, L., Serre, G., Guerrin, M. and Jonca, N. (2011). The ubiquitous dermokine delta activates Rab5 function in the early endocytic pathway. *PLoS ONE* **6**, e17816.

Leyvraz, C., Charles, R. P., Rubera, I., Guitard, M., Rotman, S., Breiden, B., Sandhoff, K. and Hummler, E. (2005). The epidermal barrier function is dependent on the serine protease CAP1/Prss8. *J. Cell Biol.* **170**, 487-496.

Li, E. R., Owens, D. M., Djian, P. and Watt, F. M. (2000). Expression of involucrin in normal, hyperproliferative and neoplastic mouse keratinocytes. *Exp. Dermatol.* **9**, 431-438.

List, K., Szabo, R., Wertz, P. W., Segre, J., Haudenschild, C. C., Kim, S. Y. and Bugge, T. H. (2003). Loss of proteolytically processed filaggrin caused by epidermal deletion of Matriptase/MT-SP1. *J. Cell Biol.* **163**, 901-910.

Matsui, T., Hayashi-Kisumi, F., Kinoshita, Y., Katahira, S., Morita, K., Miyachi, Y., Ono, Y., Imai, T., Tanigawa, Y., Komiya, T. et al. (2004). Identification of novel keratinocyte-secreted peptides dermokine-alpha/-beta and a new stratified epithelium-secreted protein gene complex on human chromosome 19q13.1. *Genomics* **84**, 384-397.

Moffatt, P., Salois, P., St-Amant, N., Gaumond, M. H. and Lanctôt, C. (2004). Identification of a conserved cluster of skin-specific genes encoding secreted proteins. *Gene* **334**, 123-131.

Naso, M. F., Liang, B., Huang, C. C., Song, X. Y., Shahied-Arruda, L., Belkowski, S. M., D'Andrea, M. R., Polkovitch, D. A., Lawrence, D. R., Griswold, D. E. et al. (2007). Dermokine: an extensively differentially spliced gene expressed in epithelial cells. *J. Invest. Dermatol.* **127**, 1622-1631.

Park, G. T., Lim, S. E., Jang, S. I. and Morasso, M. I. (2002). Suprabasin, a novel epidermal differentiation marker and potential cornified envelope precursor. *J. Biol. Chem.* **277**, 45195-45202.

Raghunath, M., Hennies, H. C., Velten, F., Wiebe, V., Steinert, P. M., Reis, A. and Traupe, H. (1998). A novel in situ method for the detection of deficient transglutaminase activity in the skin. *Arch. Dermatol. Res.* **290**, 621-627.

Rawlings, A. V. and Harding, C. R. (2004). Moisturization and skin barrier function. *Dermatol. Ther.* **17 Suppl 1**, 43-48.

Sevilla, L. M., Nachat, R., Groot, K. R., Klement, J. F., Uitto, J., Djian, P., Määttä, A. and Watt, F. M. (2007). Mice deficient in involucrin, envoplakin, and periplakin have a defective epidermal barrier. *J. Cell Biol.* **179**, 1599-1612.

Steven, A. C. and Steinert, P. M. (1994). Protein composition of cornified cell envelopes of epidermal keratinocytes. *J. Cell Sci.* **107**, 693-700.

Tagi, T., Matsui, T., Kikuchi, S., Hoshi, S., Ochiai, T., Kokuba, Y., Kinoshita-Ida, Y., Kisumi-Hayashi, F., Morimoto, K., Imai, T. et al. (2010). Dermokine as a novel biomarker for early-stage colorectal cancer. *J. Gastroenterol.* **45**, 1201-1211.

Toulza, E., Serre, G. and Guerrin, M. (2004). Towards a transcriptome definition of the fully differentiated human skin keratinocytes. *J. Invest. Dermatol.* **123**, A98.

Toulza, E., Galliano, M. F., Jonca, N., Gallinaro, H., Méchin, M. C., Ishida-Yamamoto, A., Serre, G. and Guerrin, M. (2006). The human dermokine gene: description of novel isoforms with different tissue-specific expression and subcellular location. *J. Invest. Dermatol.* **126**, 503-506.

Toulza, E., Mattiuzzo, N. R., Galliano, M. F., Jonca, N., Dossat, C., Jacob, D., de Daruvar, A., Wincker, P., Serre, G. and Guerrin, M. (2007). Large-scale identification of human genes implicated in epidermal barrier function. *Genome Biol.* **8**, R107.

Tsuchida, S., Bonkobara, M., McMillan, J. R., Akiyama, M., Yudate, T., Aragane, Y., Tezuka, T., Shimizu, H., Cruz, P. D., Jr and Ariizumi, K. (2004). Characterization of Kdap, a protein secreted by keratinocytes. *J. Invest. Dermatol.* **122**, 1225-1234.

Turksen, K. and Troy, T. C. (2002). Permeability barrier dysfunction in transgenic mice overexpressing claudin 6. *Development* **129**, 1775-1784.

Xiang, H., Feng, Y., Wang, J., Liu, B., Chen, Y., Liu, L., Deng, X. and Yang, M. (2012). Crystal structures reveal the multi-ligand binding mechanism of Staphylococcus aureus ClfB. *PLoS Pathog.* **8**, e1002751.